Determination of nanomolar concentrations of lead and cadmium by anodic-stripping voltammetry at the silver electrode

Y. Bonfil, E. Kirowa-Eisner*

School of Chemistry, Raymond and Beverly Sackler Faculty of Exact Sciences, Tel Aviv University, Tel Aviv 69978, Israel

Abstract

Lead and cadmium have been determined by subtractive anodic-stripping voltammetry (SASV) in the square-wave mode at a silver electrode without removal of oxygen. The sensitivities and detection limits for the two metals differ considerably. Detection limits of 0.05 nM for lead and 1 nM for cadmium have been achieved following 90 s electrodeposition. The repeatability of consecutive SASV runs is good (for lead 0.5% at 20 nM for 30 s electrolysis, 5% at 0.3 nM for 60 s electrolysis; for cadmium 2.5% at 20 nM for 30 s electrolysis, 5% at 5 nM for 60 s). Hundreds of runs can be carried out without any pretreatment of the electrode. The high stability is attributed to renewal of the electrode surface that takes place during the electrodeposition step in a two-electrode cell: the silver counter/quasi-reference electrode generates silver ions that codeposit with lead and cadmium at the Ag-RDE, thus ensuring a continuity of the latter. Underpotential deposition (UPD) plays a central role in anodic-stripping voltammetry (ASV). During the deposition step, the adatom coverage of trace elements is in the range of 0.01–1% and no bulk deposition is invoked for metals that exhibit UPD. The UPD properties and, as a result, the ASV signals are strongly affected by the type and concentration of the supporting electrolyte. The effects of Cl^-, Br^-, SO_4^{2-} and NO_3^- are shown. The analysis of lead and cadmium in natural waters has been performed. Surfactants distort the SASV signal. In order to ensure surfactant-free solutions, the samples were pretreated by wet ashing. © 2002 Elsevier Science B.V. All rights reserved.

Keywords: Anodic-stripping voltammetry; Silver electrode; Lead; Cadmium; Trace analysis; Background correction

1. Introduction

The most sensitive anodic stripping methods for lead and cadmium are based on mercury (2 pM following 12 min electrodeposition for lead) [1] and on glassy carbon mercury film electrodes (8 pM for lead and 5 pM for cadmium following 5 min electrodeposition) [2]. Several solid electrodes were shown to be useful for the determination of lead and cadmium in mixtures: (i) bismuth-coated carbon electrode for which only the detection limit for lead is reported (1.5 nM following 10 min deposition time) [3]; (ii) glassy-carbon disk with a detection limit of 80 nM for both lead and cadmium following 3 min deposition time [4]; (iii) silver-coated carbon electrode with a detection limit for lead of 5 nM following 2 min deposition [5]; (iv) silver electrode with a detection limit of 9 nM for cadmium and 2.5 nM for lead [6]; (v) gold has been found to be unsuitable for mixtures of lead and cadmium as a result of overlapping of the two stripping peaks [7].

In this work, detection limits of 50 pM for lead and 1 nM for cadmium have been reached with the use of a silver electrode following a deposition time of 90 s. The silver electrode exhibits excellent characteristics for lead [8]: high repeatability (better than

* Corresponding author. Tel.: +972-3640-8239;
fax: +972-3-540-6553.
E-mail address: eisner@post.tau.ac.il (E. Kirowa-Eisner).

2% at 1 nM Pb^{2+}) and long-term stability without requiring any pretreatment. The performance is less good for Cd^{2+}. Optimal environment for the analysis includes: (i) use of a non-isolated silver counter electrode and solutions from which oxygen has not been removed. This ensures continuous renewal of the silver working electrode [8]; (ii) application of subtractive anodic-stripping voltammetry (SASV), which includes correction for background [8–11]. This mode greatly improves the performance of anodic stripping analysis as can be seen from the detection limit and separation of adjacent peaks; (iii) using a two-electrode configuration in which the counter/reference electrode is a silver rod dipped directly into the test solution [8,12]. This has two advantages: first, fewer components are inserted into the cell and second, it avoids the use of a conventional reference electrode. The latter has a porous separator that may desorb impurities and is usually made of Pyrex glass, which is not suitable for the analysis of sub-nanomolar concentrations of lead because of the danger of leaching of the metals [8]; (iv) adding the standard additions in rapid sequence [8–12]. This decreases the danger of contamination and ensures smaller drifts of the background during the analysis.

Underpotential deposition (UPD) plays a central role in the deposition and dissolution steps of anodic-stripping voltammetry (ASV) [9,10,12]. Species that exhibit UPD form a monolayer of adatoms, which are deposited and stripped at potentials positive to the reversible Nernst potential. During the deposition step, the adatom coverage of trace elements is in the range of 0.01–1% and no bulk deposition is invoked for metals that exhibit UPD (e.g. Pb and Cd on Ag; Hg, Cu and Pb on Au) [9–12]. In these cases, the UPD properties of the deposit are the main factor determining the analytical characteristics of the method.

The UPD properties, and as a result, the ASV signal are strongly affected by the type and concentration of the supporting electrolyte [13]. For example, the lead signal on silver reaches its maximum at 10 mM Cl^-. In the absence of Cl^- its height is lower by a factor of 3 and remains so also in the presence of bromides, sulfates and nitrates. If only sulfates or nitrates are present, the cadmium signal on silver does not appear. A well defined peak appears in the presence of chlorides and bromides, but its intensity is one-fifth that of the lead signal.

The method has been applied to the determination of mixtures of Pb^{2+} and Cd^{2+} in natural water samples.

2. Experimental

2.1. Instrumentation

An GPES-μAutolab software (EcoChemie) and a homemade rotating disk electrode were used.

2.2. Cell

A 10 ml quartz cell was used in a two-electrode configuration. The working electrode was a homemade silver rotating electrode and the counter/reference silver quasi-reference electrode (AgQRE) [12] was a 1 cm^2 silver rod, dipped directly into the solution that contains at least 10 mM chloride ions. The potential of AgQRE in 10 mM KCl or NaCl is 98 ± 5 mV versus SCE. This potential is stable for thousands of runs. The electrode was stored in pure water and was used for months without any pretreatment. The silver chloride coating on the electrode was stripped with emery paper every thousand runs. With a three-electrode configuration (platinum as counter electrode) the functioning of the silver electrode deteriorates with time and requires frequent mechanical pretreatment. It has been speculated [8] that the reason for the high performance of the two-electrode configuration with the silver counter/reference electrode is that during the electrodeposition step, silver ions that dissolved from the counter silver electrode are uniformly redeposited on the working electrode bringing about its continuous renewal.

The simplicity of the two-electrode cell is of utmost importance for the sub-nanomolar concentration range. The preparation of the silver disk electrode, Ag-RDE, has been described in [8].

2.3. Chemicals and glassware

All solutions were prepared in type 1 reagent grade water (18.3 MΩ cm resistivity, obtained with Barnstead EASYpure^{TM}RF water purification). A 0.1 mM $Pb(NO_3)_2$ and 0.1 mM $Cd(NO_3)_2$, both in 10 mM HNO_3 were used for daily preparation of the standard solutions. HNO_3 65%, H_2SO_4, $HClO_4$, HCl,

NaCl and KCl were all Merck, Suprapur. The other chemicals were Merck, GR. Plastic ware (PTFE) and glassware were cleaned prior to use by immersion for few hours in (a) liquid cleaner (MICRO, Cole Parmer), (b) 1:1 aqueous solution of HNO_3 and rinsed by copious amounts of reagent grade water.

2.4. The ASV (classical mode) and the SASV procedures

2.4.1. ASV

The stripping step was performed in the square wave mode. The analysis was performed without removal of oxygen in a 5 ml aliquot, containing 10 mM HNO_3 and 10 mM NaCl. The ASV procedure consisted of the following steps performed in an uninterrupted sequence. (a) Conditioning of the electrode: the working electrode was rotated while applying a potential in order to destroy the diffusion layer formed from previous experiment and to ensure dissolution of remaining deposits, $E_{cond} = -0.05$ V versus AgQRE, $t_{cond} = 10$ s. The stirring of the solution during the conditioning step is of utmost importance when subsequent ASV is performed in a fast sequence. A systematic increase in the peak height was observed if this step is deleted. (b) The deposition step: E_{dep}, in the range of -0.8 to -0.65 V, depending on the ratio of concentrations of Pb^{2+} and Cd^{2+}; 15 s $\leq t_{dep} \leq 90$ s; $N = 3500$ rpm. (c) The rest step as step (b), but without rotating the electrode, $t_{rest} = 10$ s. (d) The stripping step was performed with square wave voltammetry, square-wave amplitude (peak-to-peak) $= 10$ mV; step amplitude $= 2.5$ mV, frequency $= 25$ Hz, E_{in} is in the range of -0.8 to -0.6 V, $E_f = -0.05$ V.

2.4.2. SASV

The procedure for the SASV consists of recording a classical ASV followed by a blind ASV (0 deposition time) in a non-interrupted sequence using the "project" feature of the GPES-μAutolab software. By subtracting the blind voltammogram from the normal ASV, the SASV was obtained.

2.5. Evaluation of the analytical signal of the ASV and of the SASV

The sum of the absolute values of the slopes at the two inflection points of the peak was used as measure for the analytical signal of the anodic stripping voltammogram. It was shown in previous works [8–11] that the slope at the inflection point is best suited when the base line is asymmetric around the peak. The slope is independent of the way the background is chosen, while the peak current or the charge are strongly dependent on it.

2.6. Construction of standard addition curves and calibration curves

The curves were constructed in a rigid, non-interrupted sequence using the "project" feature of the GPES-μAutolab software. Performing the standard additions in the shortest possible time is of utmost importance in the nanomolar and sub-nanomolar concentration range. Keeping the time of analysis short decreases the chances of (a) contamination of the test solution, (b) changes in the magnitude of the signal due to temperature variations and (c) changes in the response of the electrode. Each new aliquot of the sample was introduced immediately after the recording of the previous curve.

The quantitative determinations were performed using the standard additions method.

2.7. Pretreatment of drinking waters samples

Water samples were acidified to pH 2 with nitric acid immediately after collection. Pretreatment of the sample is necessary in order to destroy organic complexants and organic surfactants. The most common procedures are based on wet digestion and UV irradiation. The on-line UV method is fast and efficient [14], but the frequently used batch mode, requires many hours of irradiation. The pretreatment procedure based on wet ashing used in this work was that described in [8]. The samples were analyzed within 1 h of collection.

3. Results and discussion

3.1. The subtractive anodic stripping voltammetric method, SASV

The efficiency of the background correction achieved by the SASV method proposed by us has
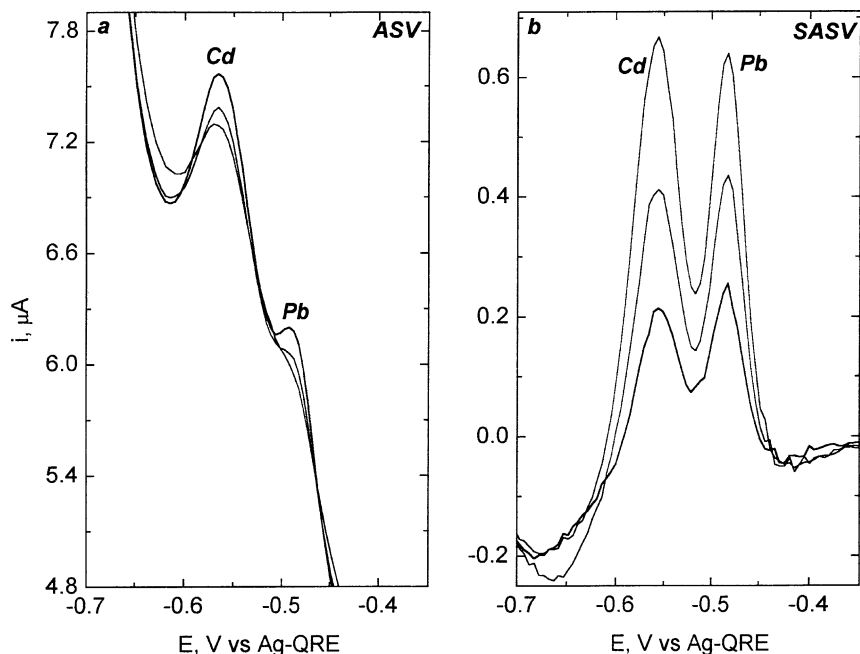
Fig. 1. Anodic stripping voltammograms (ASV) (a), and subtractive anodic stripping voltammograms (SASV) (b) at Ag-RDE without removal of oxygen. 2, 4, 6 nM Pb^{2+} and 10, 20 and 30 nM Cd^{2+} in 10 mM HNO_3, 10 mM NaCl. Conditions for electrodeposition: E_{dep} = −0.8 V; t_{dep} = 30 s; rotating rate = 3500 rpm. Square-wave mode: square-wave amplitude 10 mV; step amplitude 2.5 mV; frequency 25 Hz.

been shown in the determination of lead, copper and mercury [8–11].

The application of SASV for the determination of mixtures of Pb^{2+} and Cd^{2+} is of utmost importance due to (i) the proximity of their peaks and (ii) the steep background caused by the reduction of nitrates, the latter catalyzed by adatoms of cadmium [15]. With the classical ASV method the two peaks are not well defined (Fig. 1a), while with the SASV method the display is dramatically improved. Another important feature of the SASV is that the determination can be carried out without the removal of oxygen: the distortion caused by the oxygen at the ASV mode disappears with the SASV mode (cf. Fig. 2 in [8]).

The principle of the SASV is in performing a background correction by subtracting from the classical ASV trace the pseudo background voltammogram recorded in succession. The pseudo background is obtained by recording an ASV with 0 deposition time immediately after the original ASV. The two ASV curves are recorded in a continuous sequence using the "project" feature of the GPES-μAutolab-software.

The pseudo background curve enables a better representation of the state of the electrode than a conventional background curve taken in the supporting electrolyte only, because the variations, which can occur on the electrode during solution exchange, are considerably larger than those occurring with the recording of the pseudo background without changing the solution. The improvement achieved by the SASV can be seen in Fig. 1b. All the measurements throughout this work were performed by SASV.

3.2. Effect of anions on the analytical signal

The anodic stripping voltammograms of lead were shown to be governed by the phenomenon of UPD [12] (the deposition and dissolution peaks appear at potentials several hundred of millivolts more positive than the reversible Nernst potential of the system). The same holds also for cadmium. Since UPD is strongly affected by the concentration and the type of the anion, we tested the effect of chlorides, bromides,
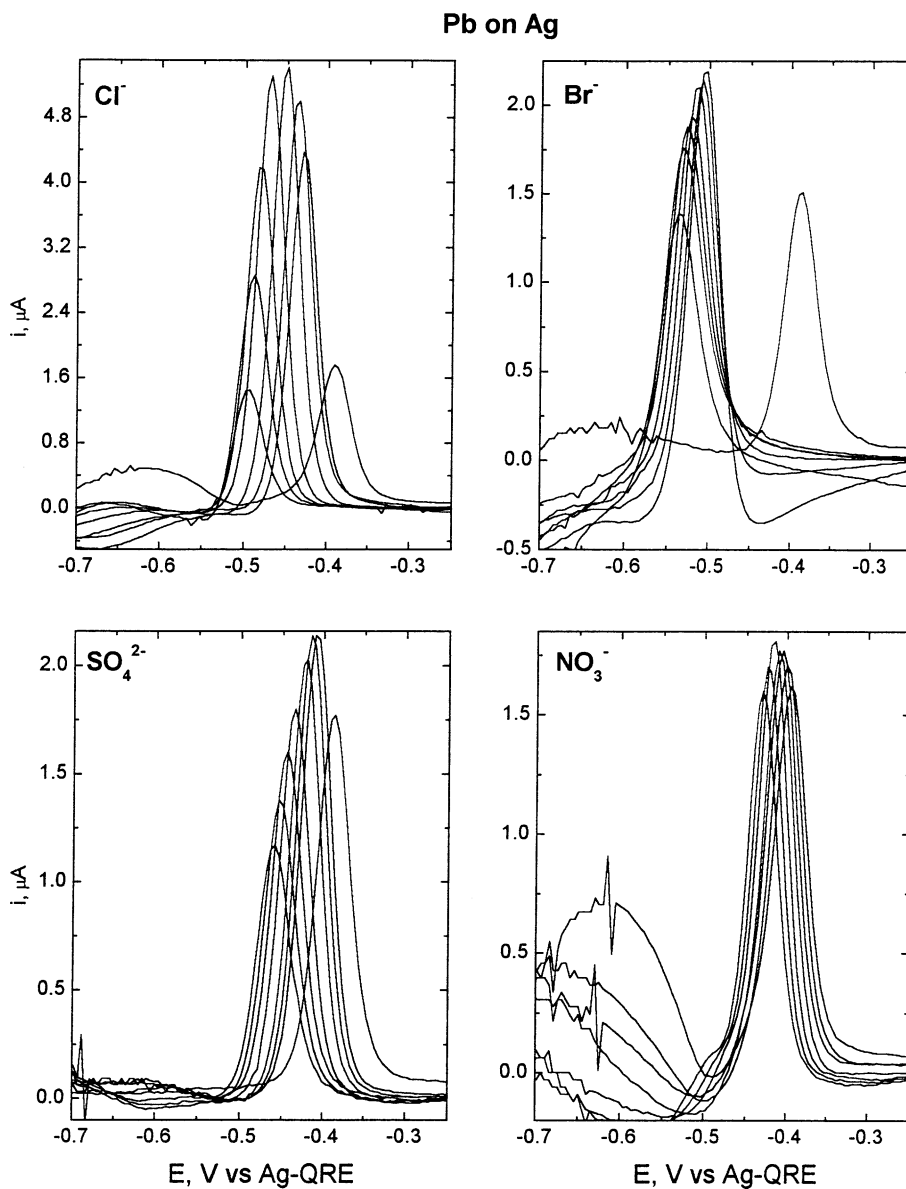
Pb on Ag

Fig. 2. SASV plots of 60 nM Pb^{2+} in 10 mM HNO_3 and different concentrations of NaCl, NaBr, Na_2SO_4 and $NaNO_3$ (from right to left): 0, 2, 4, 10, 18, 36, 70, 130 mM. The SASV plots are performed under conditions defined in Fig. 1.

sulfates and nitrates in solutions containing 10 mM HNO_3 (Figs. 2 and 3).

3.2.1. Effect on lead

In the absence of added anions only a wide and relatively low peak is displayed at −0.38 V. The effect of Cl^-, Br^-, SO_4^- and NO_3^- was tested. In all cases the peak height is dependent on concentration of the anions and except for nitrates, where the effect is small, the peak potential is shifted to increasingly negative potentials with the concentration of the electrolyte. The maximal value for the peak is reached at 10 mM for Cl^-, 2 mM for Br^-, 2 mM for SO_4^-, 10 mM for NO_3^-. At optimal anion concentration, the peak of
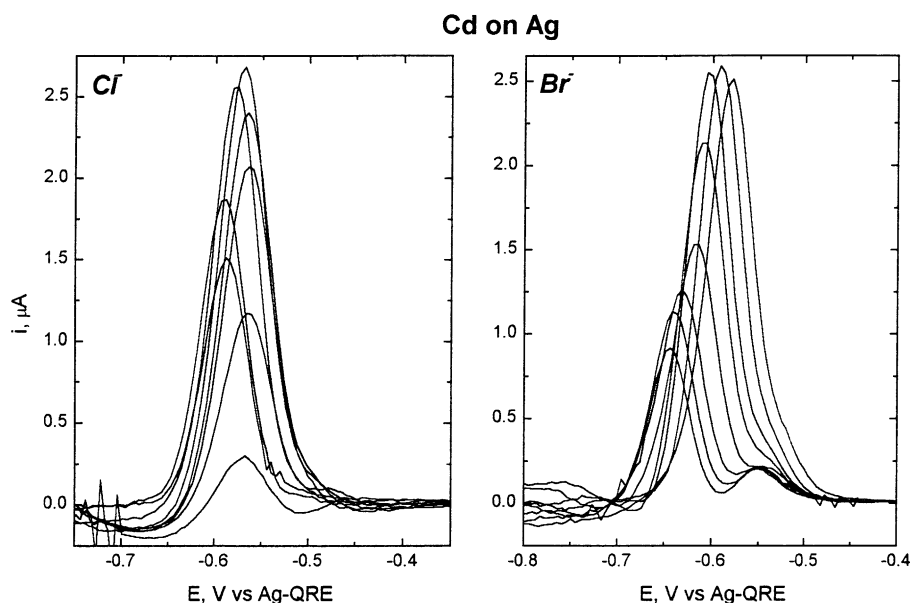
Cd on Ag

Fig. 3. SASV plots of 100 nM Cd^{2+} in 10 mM HNO_3 and different concentrations of NaCl and NaBr (from right to left): 2, 4, 6, 8, 10, 20, 38, 74 mM. The SASV plots are performed under conditions defined in Fig. 1.

lead in presence of Cl^- is higher compared to the other anions by a factor of at least 2.5.

3.2.2. Effect on cadmium

The cadmium signal on silver does not appear in 10 mM HNO_3 if only sulfates and nitrates are present.

A well-defined peak appears in the presence of chlorides and bromides. As in the case of lead, the peak potential is shifted to increasingly negative potentials with the concentration of the electrolyte. The maximal values of the signal are reached at 10 mM for Cl^-, or 4 mM for Br^-. The intensity of the cadmium
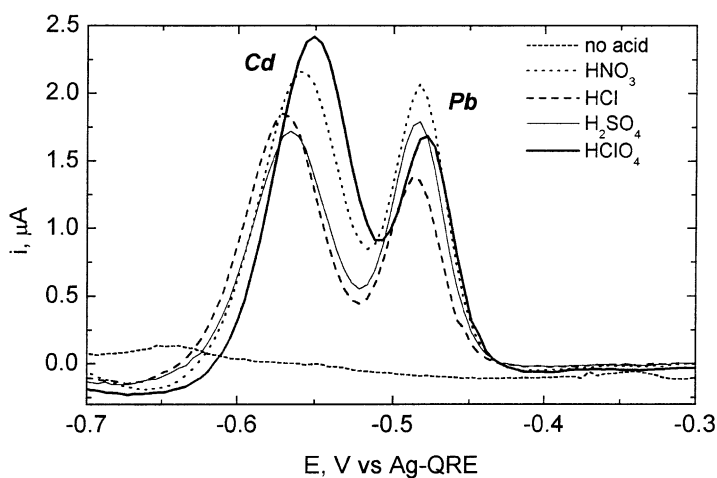

Fig. 4. SASV plots of 20 nM Pb^{2+} and 100 nM Cd^{2+} in 10 mM NaCl and 10 mM acid (type of acid is marked on the plot). The SASV plots are performed under conditions defined in Fig. 1.

signal is five times lower compared to that of lead at the respective optimal concentrations of chlorides and bromides.

The effect of anions on mixtures of cadmium and lead is identical to that of solutions of the individual metals. Chloride is the most suitable anion for the simultaneous determination of Pb^{2+} and Cd^{2+} in view of optimal sensitivity and half-peak width.

3.3. Effect of the type of acid on the analytical signal

The effect of the type of acid on the SASV signals of lead and cadmium was tested in solutions containing 10 mM NaCl. The most striking feature is that no signal of Pb^{2+} and Cd^{2+} was obtained in absence of acids. The optimal concentration range of nitric acid
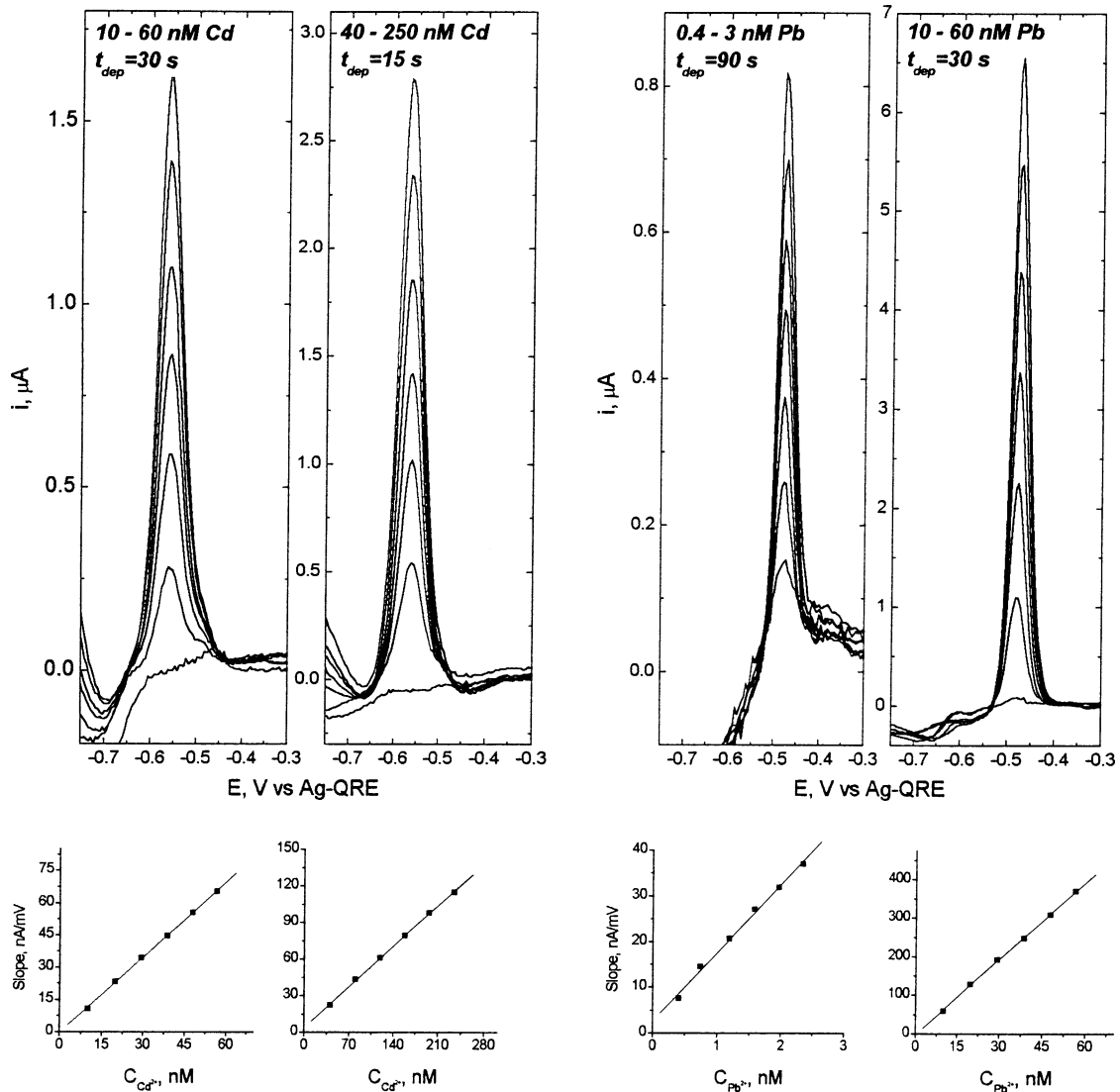

Fig. 5. SASV of Pb^{2+} and Cd^{2+} at the Ag-RDE and the respective calibration curves. The values in the calibration curves are corrected for the respective blanks. Supporting electrolyte: 10 mM HNO_3, 10 mM NaCl. Deposition time as marked on plots. Other conditions same as in Fig. 1.

in view of the peak height is 2–10 mM. The SASV signals in presence of different acids are displayed in Fig. 4. All four acids are suitable. With nitric acid the response of Pb is the largest. With sulfuric acid the separation of the peaks is somewhat better. All analytical measurements in this work were performed in an electrolyte containing 10 mM HNO_3 and NaCl.

3.4. Analytical characteristics

SASV curves of Pb^{2+} and Cd^{2+} and their respective calibration plots are shown in Fig. 5. The peaks for lead are narrower and substantially higher than those of cadmium. Plots of mixtures with equimolar concentrations of Pb^{2+} and Cd^{2+} (Fig. 6) clearly show the difference between the responses of the two ions. The obvious result is that the detection limit for Cd^{2+} is considerably higher. Concentrations of Pb^{2+} as low as 0.5 nM can be determined at 90 s deposition time, while the lowest concentration of Cd^{2+} at the same deposition time is about 5 nM. The locations of the peaks

are independent of concentration of analyte. The half peak widths for Pb^{2+} and Cd^{2+} are 35 and 50 mV, respectively. The detection limits for Pb^{2+} and Cd^{2+} are 0.05 and 1 nM, respectively at 90 s deposition time and 3500 rpm rotation rate.

The proximity of the two peaks poses a problem in the analysis of mixtures with large excess of one of the components. Large excess of lead distorts the descending (the more anodic) branch of the cadmium peak. The analysis of cadmium can be carried out in the presence of a five-fold excess of lead (Fig. 7a). The excess of lead can be even larger if the mode of measurements of the analytical signal is modified by measuring the slope at the inflection point of the rising part of the peak only instead of the sum of the slopes of both the rising and the descending branches. Analysis of Pb^{2+} in excess Cd^{2+} is a much easier task. The determination of Pb^{2+} can be carried out by performing the deposition step at a potential at which cadmium is not deposited and thus does not interfere. An example is given in Fig. 7b. The signal of Pb is heavily perturbed by the presence of large excess of Cd if a deposition potential at which both metals are deposited is applied. However, changing the deposition potential to −0.65 V yields well-defined signal for lead, totally unperturbed by the cadmium (Fig. 7c).

Linear relationship of signal/concentration (0.4–300 nM for lead and 5–250 nM for cadmium) and signal/deposition time (tested range 15–120 s) at 3500 rpm is observed in solutions of Pb^{2+}, of Cd^{2+} and of their mixtures. Calibration plots at large concentration ranges and at different deposition times are presented in Fig. 8. The correlation coefficients of the respective linear parts are higher than 0.999. The plots start to deviate from linearity at about a constant value for the analytical signal (500 and 120 nA mV^{-1} for Pb^{2+} and Cd^{2+}, respectively). Since the analytical signal is proportional to the product $C_{M^{2+}} N^{1/2} t_{dep}$, it is estimated that deviation from linearity occurs when this product equals to 2×10^5 nM rpm$^{1/2}$ s $\pm 10\%$. The electrode coverage by the deposited metals at the break point corresponds to a coverage of about 1% of monolayer (taking into account the roughness factor of the silver electrode as 2.6 and using Levich equation for estimation the limiting current at which the ions are deposited [12]). Breaking points of this type have been observed also for Hg^{2+} and Cu^{2+} at gold electrodes at coverages corresponding to 5% of monolayer.
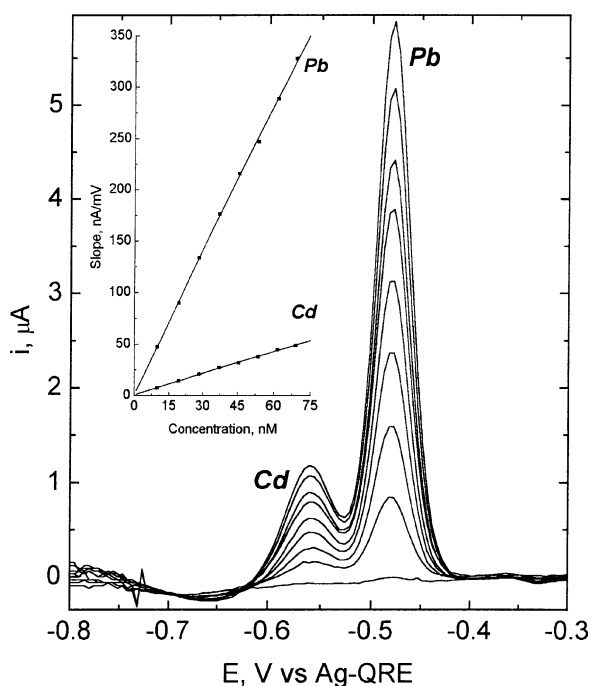

Fig. 6. SASV at equimolar concentrations of Pb^{2+} and Cd^{2+} at the Ag-RDE without removal of oxygen and the respective calibration curves. Supporting electrolyte: 10 mM HNO_3, 10 mM NaCl. The SASV plots are performed under conditions defined in Fig. 1.
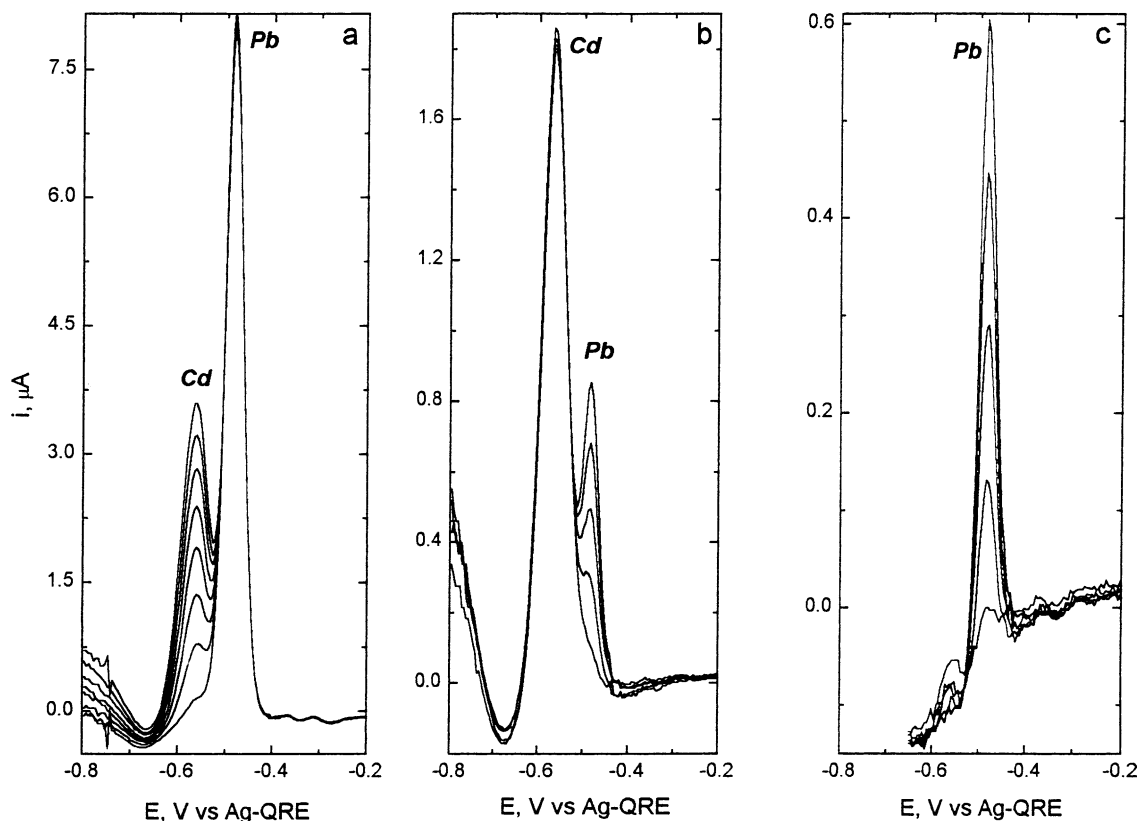
Fig. 7. SASV of Pb^{2+} and Cd^{2+} at the Ag-RDE in 10 mM HNO$_3$, 10 mM NaCl. (a) [Pb^{2+}] = 100 nM; [Cd^{2+}] = 27 nM; 54, 81, 108, 135, 161, 187, 213 nM; E_{dep} = −0.8 V. (b) [Pb^{2+}] = 2.0 nM; 3.95, 5.9, 7.85 nM; [Cd^{2+}] = 100 nM; E_{dep} = −0.8 V. (c) [Pb^{2+}] = 2.0 nM; 3.95, 5.9, 7.85 nM; [Cd^{2+}] = 100 nM; E_{dep} = −0.0.65 V. All other conditions same as in Fig. 1.

The sensitivity of the signal is 50 ± 5 and 10 ± 1 AV^{-1} cm^{-2} M^{-1} s^{-1} rpm$^{-1/2}$ for lead and cadmium, respectively.

3.5. Interferences

3.5.1. Organic surfactants and organic complexants

Organic surfactants and organic complexants are a serious interference due to fouling of the silver working electrode and bounding the metals in organic complexes and have to be removed prior to analysis. The first run in an unpretreated sample has usually a normal shape, which deteriorates rapidly in subsequent runs (Fig. 9a). Polishing of the electrode restores its proper functioning. After applying the pretreatment of the wet ashing method used by us in previous

work [8], highly reproducible signal were produced (Fig. 9b) and no repolishing of the electrode was needed.

3.5.2. Oxygen

Somewhat distorted signals with the classical ASV were obtained in samples in which oxygen was not removed. With the SASV mode, however, signals in presence and in absence of oxygen were identical.

3.5.3. Copper

Copper is of importance due to its abundance in water samples. The stripping peak of Cu^{2+} at the Ag electrode is displayed at about 0 V versus AgQRE. It is ill defined and is not suitable for analytical determination. Large excess of copper might cause
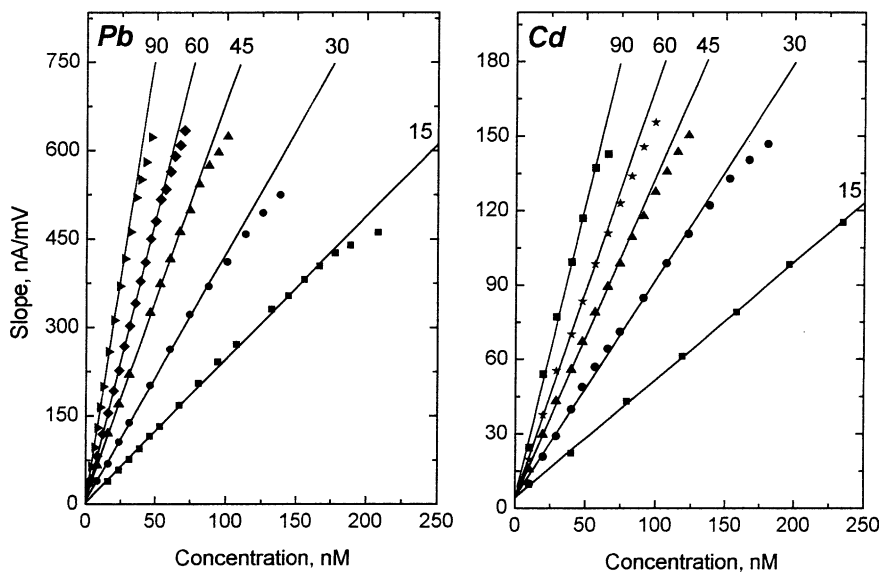
Fig. 8. SASV calibration plots for Pb^{2+} and Cd^{2+} at the Ag-RDE for different deposition times, as marked on plots. The SASV plots are performed under conditions defined in Fig. 1.
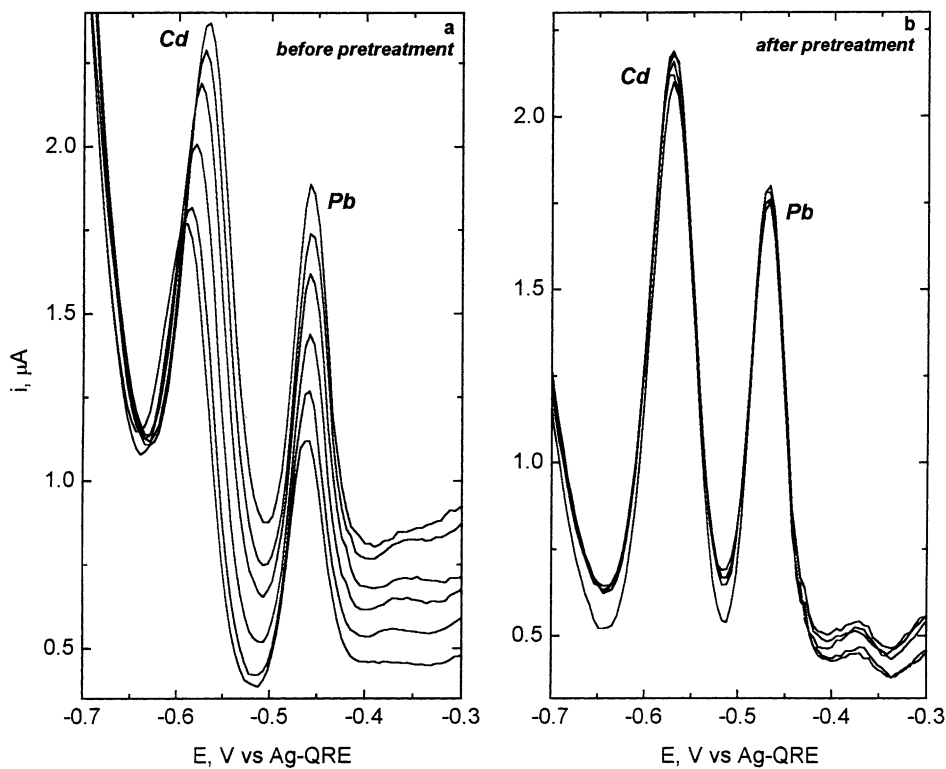

Fig. 9. Effect of pretreatment of drinking water on the stability of the SASV plots at the Ag-RDE. Supporting electrolyte: 10 mM HNO_3, 10 mM NaCl. The SASV plots are performed under conditions defined in Fig. 1.

change in the surface of the electrode, thus affecting the signals of lead and cadmium. Peak location, peak sensitivity, and peak width of lead and cadmium are however unaffected by the presence of 0.2 mM Cu^{2+} (up to 50,000-fold excess in the case of lead and up to 10,000 in the case of cadmium).

The lack of interference of large excess of Cu^{2+} in the determination of nanomolar concentrations of Pb^{2+} and Cd^{2+} may be due to formation of a sub-monolayer of lead and cadmium attached directly to the surface of the silver, with the copper growing as a three-dimensional nuclei that occupies the free parts of the electrode. (The coverage of lead and cadmium, deposited from nanomolar concentrations of Pb^{2+} and Cd^{2+}, amounts to less than 1% of the electrode surface, as determined in this work.) Were lead, cadmium and copper deposited randomly on the electrode, the lead would be trapped in the copper deposit and a decrease in the stripping peak height with increase of concentration of Cu^{2+} would be observed. There are two observations supporting the model of submonolayer of lead and cadmium and dendrite formation of copper. (i) Copper is not deposited at underpotential on silver [13], and thus the copper deposits in a three-dimensional nuclei of pure copper, occupying a small fraction of the surface, leaving enough space for submonolayer deposition of Pb and Cd. (ii) Lead and cadmium are deposited on copper at an underpotential shift larger by 100 mV than that on silver ([13], p. 158). The experimental findings are that the peak potential of SASV of Pb^{2+} and Cd^{2+} are independent of the presence of the copper deposit. This indicates that the lead and cadmium are deposited on silver and not on the copper deposit.

The difference in the permissible excess of copper in the analysis of lead and of cadmium is of interest. The smaller permissible excess of copper in the case of cadmium is due to the electrocatalytic reduction of nitrates in the presence of copper [15]. The reduction wave of nitrates is shifted to positive potentials with increasing concentrations of copper till it overlaps with the dissolution wave of cadmium. (Both waves exhibit positive currents due to the fact that a square-wave signal represents the difference between the forward and backward components of the current.) This type of interference can be overcome by replacing the nitric acid in the supporting electrolyte with sulfuric or perchloric acids.
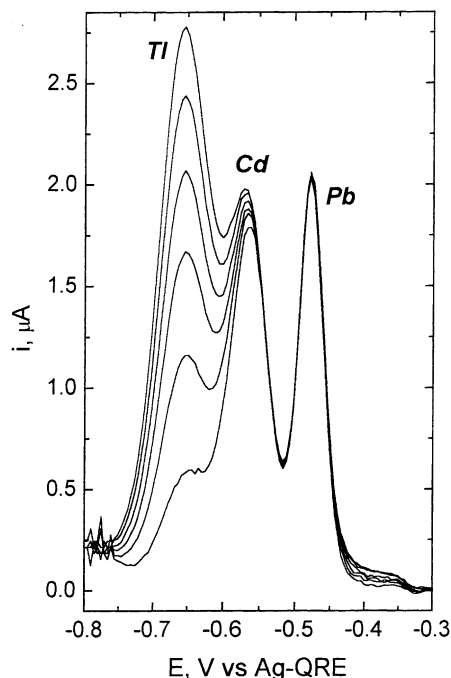

Fig. 10. SASV plots of 20 nM Pb^{2+} and 100 nM Cd^{2+} in the presence of increasing concentrations of Tl^+: 0.20, 0.39, 0.59, 0.78, 0.97, 1.17 μM. Supporting electrolyte: 10 mM HNO_3, 10 mM NaCl. The SASV plots are performed under conditions defined in Fig. 1.

3.5.4. Thallium

The anodic stripping peak of thallium is displayed at potential slightly more negative than that of the cadmium peak. The sensitivity of the peak of thallium in the supporting electrolyte used in this work is very low (Fig. 10) and thus only high concentrations of thallium interfere with the determination of cadmium, but not with that of lead.

3.6. Determination of Pb^{2+} and Cd^{2+} in drinking water

The electrochemical determination of metal ions may be affected by the presence of organic matter in samples due to changes in concentration of free metal ions (formation of complexes) and modification of the electrode surface (adsorption on the surface). The pre-treatment applied in this work followed the wet ashing method (Section 2.7) used in the determination of lead in [8].
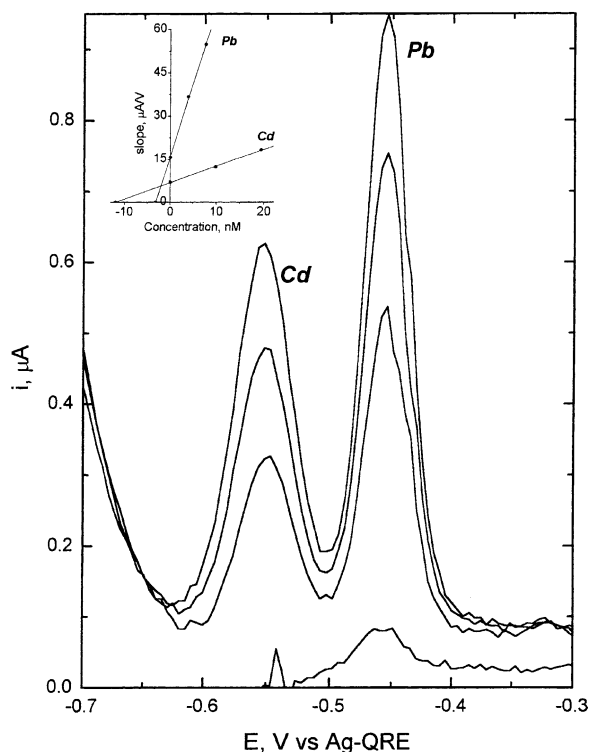
Fig. 11. Determination of Pb^{2+} and Cd^{2+} in water from cooler sample using the method of standard addition. The sample was pretreated and prepared according to Section 2.7. Each standard addition consists: 20 µl, 1 µM Pb^{2+} and 50 µl, 1 µM Cd^{2+} into 4 ml sample. Supporting electrolyte: 10 mM HNO_3, 10 mM NaCl. Conditions for square-mode same as in Fig. 1.

The validity of the wet ashing method was tested by the degree of recovery of lead and cadmium from synthetic solutions. Three sets of duplicates of a solution containing 50 nM of Pb^{2+} and Cd^{2+} were tested using the standard additions method. The average recovery was $101\% \pm 5$ for Pb^{2+} and $102\% \pm 6$ for Cd^{2+}.

Lead and cadmium were simultaneous determined in tap water and in water from a cooler (Fig. 11), both collected at Tel Aviv University. The results, based on the analysis of six samples from each source, are as follows: tap water $12 \pm 0.5\,\mu g\,l^{-1}$ Pb^{2+} and $< 2\,\mu g\,l^{-1}$ Cd^{2+}; water from cooler $2.9 \pm 0.2\,\mu g\,l^{-1}$ Pb^{2+} and $5.5 \pm 0.2\,\mu g\,l^{-1}$ Cd^{2+}. Samples from

the cooler were analyzed by ICP by an independent and certified analytical laboratory. The results for lead and cadmium were $3 \pm 1\,\mu g\,l^{-1}$ Pb^{2+} and $4.7 \pm 1\,\mu g\,l^{-1}$ Cd^{2+}. The discrepancy between the SASV and ICP results is due to the low accuracy of ICP at that concentration level of lead and cadmium. The analysis of a synthetic solution with higher concentration ($10\,\mu g\,l^{-1}$ Pb^{2+} and $25\,\mu g\,l^{-1}$ Cd^{2+}), showed agreement between the two methods to within 10%.

Acknowledgements

References

[1] L. Mart, H.W. Nurenberg, P. Valenta, Fres. Z. Anal. Chem. 300 (1980) 350.
[2] E. Fischer, C.M.G. van den Berg, Anal. Chim. Acta 385 (1999) 273.
[3] J. Wang, J. Lu, S.B. Hocevar, P.A.M. Farias, Anal. Chem. 72 (2000) 3218.
[4] J.F. van Staden, M.C. Matoetoe, Anal. Chim. Acta 411 (2000) 201.
[5] O. Bagel, G. Lagger, H.H. Girault, D. Brack, U. Loyall, H. Schafer, Electroanalysis 13 (2000) 100.
[6] O. Mikkellse, K.H. Schroder, Electroanalysis 13 (2001) 687.
[7] J. Wang, B. Tian, Electroanalysis 5 (1993) 809.
[8] E. Kirowa-Eisner, M. Brand, D. Tzur, Anal. Chim. Acta 385 (1999) 325.
[9] Y. Bonfil, M. Brand, E. Kirowa-Eisner, Anal. Chim. Acta 387 (1999) 85.
[10] Y. Bonfil, M. Brand, E. Kirowa-Eisner, Anal. Chim. Acta 424 (2000) 65.
[11] Y. Bonfil, M. Brand, E. Kirowa-Eisner, Rev. Anal. Chem. 19 (2000) 201.
[12] M. Brand, I. Eshkenazi, E. Kirowa-Eisner, Anal. Chem. 69 (1997) 4660.
[13] D.M. Kolb, in: H. Gerischer, C.W. Tobias (Eds.), Advances in Electrochemistry and Electrochemical Engineering, Vol. 11, Wiley, New York, 1978.
[14] E.P. Achtenberg, C.M.G. van den Berg, Anal. Chim. Acta 291 (1994) 213.
[15] X. Xing, D.A. Scherson, Anal. Chem. 59 (1987) 962.